

## High-temperature structural evolution of caesium and rubidium triiodoplumbates

D. M. Trots<sup>1,\*</sup>, S. V. Myagkota<sup>2,3</sup>

<sup>1</sup> HASYLAB at DESY, Notkestraße 85, 22607 Hamburg, Germany

<sup>2</sup> Physics Department, Ivan Franko National University of Lviv, 8 Kyryla i Mefodiya Str., 79005 Lviv, Ukraine

<sup>3</sup> Lviv State Agrarian University, 1 Volodymyra Velykogo Str., 80381 Dublyany-Lviv, Ukraine

### Abstract

CsPbI<sub>3</sub> and RbPbI<sub>3</sub> were investigated by *in situ* powder diffraction within temperature ranges of 298—687 K and 298—714 K, respectively. Both compounds crystallize in orthorhombic *Pnma* symmetry and expand isotropically upon a heating, revealing almost the same relative change of the lattice parameters. A pronounced difference in the structural evolution close to 600 K was observed, namely, CsPbI<sub>3</sub> undergoes first order reversible phase transformation  $Pnma \xleftarrow{563K} Pnma + Pm\bar{3}m \xleftarrow{602K} Pm\bar{3}m$ , whereas no transitions (except of the sample's melting) in RbPbI<sub>3</sub> were detected. An attempt to clarify the relation between the existence/absence of a phase transition and bulging out of the iodine environment around alkaline ions was undertaken.

**Keywords:** C. X-ray diffraction, D. crystal structure, D. phase transitions, D. thermal expansion

---

\* CORRESPONDING AUTHOR. Tel. +49-40-8998-2918, Fax: +49-40-8998-2787,

e-mail: [d.trots@yahoo.com](mailto:d.trots@yahoo.com)

## Introduction

Optical properties of caesium and rubidium triiodoplumbates have been extensively studied [1, 2] since their implementation as scintillators is of considerable interest [3].

The structure of caesium triiodoplumbate was originally determined by Møller [4]. However, the accuracy of his work was limited by the experimental technique available at that time. The structure of rubidium triiodoplumbate at room temperature was precisely determined by single crystal diffraction [5]: RbPbI<sub>3</sub> crystallizes in the orthorhombic symmetry *Pnam* with  $a = 10.274(1)$  Å,  $b = 17.381(2)$  Å,  $c = 4.773(1)$  Å,  $Z = 4$  and is isomorphous with CsPbI<sub>3</sub>. The Pb<sup>2+</sup> ions are surrounded octahedrally by I in this structure. The PbI<sub>6</sub>-octahedra are arranged in the double chains along the *c*-axis that are held together by alkaline ions [5]. CsPbI<sub>3</sub> and RbPbI<sub>3</sub> belong to the structure type of NH<sub>4</sub>CdCl<sub>3</sub>/Sn<sub>2</sub>S<sub>3</sub>.

To our knowledge, there are no data on the high-temperature structural evolution of CsPbI<sub>3</sub> and RbPbI<sub>3</sub> in the literature. The analysis of the results presented in [4] shows that more accurate structural studies of caesium triiodoplumbate are of interest. This requires a more accurate determination of the interatomic distances in the CsPbI<sub>3</sub> structure which is the experimental basis for further understanding the correlation between optical and structural properties. Therefore, in the present work we report the results of powder diffraction studies on CsPbI<sub>3</sub> and RbPbI<sub>3</sub> within temperature ranges of 298—687 K and 298—714 K, respectively.

## Experimental

The samples were grown by the Bridgman technique in Lviv [2]. *In situ* diffraction studies at high temperatures were performed at the synchrotron facility HasyLab/DESY (Hamburg, Germany) with the powder diffractometer at beam-line B2 [6]. The 0.3×80 mm quartz capillaries were completely filled with powder samples in air and sealed. Subsequently, the capillaries were mounted in Debye-Scherrer geometry inside a STOE furnace which is equipped with a EURO THERM temperature controller and a capillary spinner. The furnace temperature was measured by a Pt10%Rh/Pt-thermocouple calibrated using the thermal expansion of NaCl. The wavelength of 0.49328 Å was selected from the direct white synchrotron radiation beam using a Si(111) double flat-crystal monochromator and determined from 8 reflection positions of LaB<sub>6</sub> reference material (NIST SRM 660a). The beam size of 0.4×3 mm at the sample position was cut

by the slits. All diffraction patterns have been collected at stabilized temperatures during the heating cycle using an image-plate detector [7] ( $2\theta$  range 4-45°). Additional check patterns were taken after the thermal treatment when the samples were cooled down to 298 K. The data evaluation was performed using the "WinPLOTR" [8] software package.

## Results

The series of measurements was initially carried out for caesium triiodoplumbate in the 298-770 K temperature range. A change of the sample colour from yellow to dark yellow was observed at the end of thermal treatment during the *in-situ* diffraction study. This can be considered as an evidence for the sample decomposition at high temperatures in air. In order to avoid the sample decomposition, the upper temperature limit was reduced down to 687 K. The additional diffraction check-pattern was collected after the sample was cooled down to 298 K. The colour changes were not revealed for CsPbI<sub>3</sub> after its heating up to 687 K, and no difference was observed in the cell volume of CsPbI<sub>3</sub> before (892.660(43) Å<sup>3</sup>) and after (892.701(49) Å<sup>3</sup>) such heat treatment. The Rietveld refinement for CsPbI<sub>3</sub> at 298 K was based on the structure model for a RbPbI<sub>3</sub> single crystal [5]. The Rietveld refinement results are presented in figure 1 and the respective values for the structural parameters are summarized in the table 1. The structure is illustrated in figure 2a. The Pb<sup>2+</sup> ions are located inside the distorted iodine octahedra exhibiting two pairs of equatorial Pb-I distances (3.2259(25) and 3.2775(25) Å) and two apical ones (3.0513(40) and 3.4076(39) Å). The alkaline ion possesses more irregular 9-fold iodine environment, namely, the three pair of iodine at the distances 3.8832(37), 3.8968(35), 3.9312(38) Å and three single iodine atoms at distances 4.0086(47), 4.0271(46), 4.1230(45) Å (figure 2b).

Besides the reflections from the orthorhombic CsPbI<sub>3</sub> phase, additional Bragg peaks arise in the diffraction patterns of CsPbI<sub>3</sub> at temperatures above 563 K. The phase transition has been found to occur within a temperature range of 563-602 K (figure 3) where the reflections from different structure modifications are present in the CsPbI<sub>3</sub> diffraction patterns. The reflections only from the high-temperature modification of CsPbI<sub>3</sub> are present in the pattern at 609 K. The analysis of the reflection indices in the high resolution synchrotron diffraction data sets collected above 602 K clearly shows that this new high temperature phase exhibits cubic symmetry (space group  $Pm\bar{3}m$ ,  $Z=1$

and  $a=6.28940(19)$  Å at 634 K). Thereafter, the structural parameters of the high-temperature modification of CsPbI<sub>3</sub> were refined on the basis of the ideal perovskite structural model (see figure 1 and table 1). In the ideal perovskite structure of the high-temperature modification of CsPbI<sub>3</sub>, twelve equal Cs–I (4.4473 Å at 634 K) and six Pb–I (3.1447 Å at 634 K) distances are observed. The PbI<sub>6</sub> octahedra are regular, and octahedral axes are parallel to the four-fold  $[0\ 0\ 1]_p$  axes of the cubic perovskite cell.

The structure of the high-temperature CsPbI<sub>3</sub> modification is illustrated in figure 2c. It reveals a large-amplitude anisotropic thermal vibration of the iodine atoms in the (100) planes. This finding possibly indicates a disorder of iodine in the Cs<sup>+</sup>–I planes. In order to achieve the best fit possible we also performed a structure refinement which additionally took the disordered iodine into account. The iodine atoms in 3(d) at  $(\frac{1}{2}, \frac{1}{2}, \frac{1}{2})$  sites were distributed along the  $\langle 100 \rangle$  directions over the 12(h) at  $(\frac{1}{2}, x, 0)$  with  $x \approx 0.09$  sites in Cs<sup>+</sup>–I plane. Although the convergence of the refinement was attained for this model, the resulting residuals were  $R_B=7.5\%$ ,  $R_F=7.2\%$  and  $\chi^2=11.4$ , compared to  $R_B=6.43\%$ ,  $R_F=6.28\%$  and  $\chi^2=11.5$  for the refinement with single-site I<sup>-</sup> ions. Therefore, the preference was given for the model with single-site I<sup>-</sup> ions, since it gives a better structural description of CsPbI<sub>3</sub> than the disordered model. We suggest that single-crystal measurements of the high-temperature polymorphous modification of CsPbI<sub>3</sub> and subsequent structure refinement including anharmonic terms in the structural model would provide more information about the nature of unusual thermal vibrations of iodine. Any ‘single-crystal’ studies are, however, practically impossible (or at least extremely difficult) even if single crystals are available, since the first order orthorhombic  $\leftrightarrow$  cubic phase transition in CsPbI<sub>3</sub> will lead to fracture (the large volume change of about 6.9% was observed upon this transition). Caesium atoms exhibit large isotropic vibrations in the high-temperature structure of CsPbI<sub>3</sub>. The similar large amplitudes of isotropic thermal vibrations for the Cs<sup>+</sup> cation and the very unusual thermal vibrations of the halogen ion in the Cs<sup>+</sup>–X<sup>-</sup> plane were discussed for the cubic perovskite phases of CsPbCl<sub>3</sub> and CsPbBr<sub>3</sub> [9].

The calculated and experimental diffraction patterns for RbPbI<sub>3</sub> are presented in figure 1. The Rietveld refinement was based on the model from reference [5]. The analysis of the structural evolution of RbPbI<sub>3</sub> above 298 K does not reveal any phase transition up to 634 K. Further heating up to 714 K leads to the escape of Bragg peaks from the diffraction pattern, *i.e.*, the melting of RbPbI<sub>3</sub> sample occurs between 634 and 714 K. The cell volume of  $854.261(85)$  Å<sup>3</sup> has been determined at room temperature for

RbPbI<sub>3</sub> recrystallized during the *in situ* diffraction experiment. This value agrees with the initial RbPbI<sub>3</sub> cell volume of 854.23(12) Å<sup>3</sup>. The refined structural parameters of RbPbI<sub>3</sub> at 298 and 634 K are summarized in table 1. The coordinations of alkaline and Pb<sup>2+</sup> ions in orthorhombic structures are illustrated in figure 2b. Bond distances and angles of RbPbI<sub>3</sub> and both polymorphous of CsPbI<sub>3</sub> are presented in table 2.

The temperature dependencies of the CsPbI<sub>3</sub> and RbPbI<sub>3</sub> cell parameters are presented in figure 3. The values of the lattice parameters increase linearly without any anomalous deviation for both CsPbI<sub>3</sub> and RbPbI<sub>3</sub> while the temperature changes within 298-687 K range. The relative changes of the cell parameters and volumes in the orthorhombic triiodoplumbates (figure 4) have been calculated in the respective temperature ranges as  $\eta x(T) = 100\% \times (x(T) - x(298 \text{ K}))/x(298 \text{ K})$ , where  $x$  corresponds to  $a$ ,  $b$ ,  $c$  and  $V$  parameters. Both CsPbI<sub>3</sub> and RbPbI<sub>3</sub> samples show the linear isotropic thermal expansion within orthorhombic phases. Furthermore, the volumetric relative expansion is almost the same for caesium and rubidium triiodoplumbates. The volume thermal expansion coefficients were calculated from the temperature dependences of the unit cell volume as  $(1/V_0) \times (dV/dT)$ , where  $(dV/dT)$  is the change of the volume in the corresponding temperature interval and  $V_0$  is the volume at the reference temperature  $T_0$  ( $T_0 = 298 \text{ K}$  in the case of orthorhombic CsPbI<sub>3</sub> and RbPbI<sub>3</sub> and  $T_0 = 609 \text{ K}$  for cubic CsPbI<sub>3</sub>). In this way, the volume thermal expansion coefficients of  $11.8 \times 10^{-5}$ ,  $11.8 \times 10^{-5}$  and  $11.9 \times 10^{-5} \text{ K}^{-1}$  have been calculated for orthorhombic CsPbI<sub>3</sub>, cubic CsPbI<sub>3</sub> and orthorhombic RbPbI<sub>3</sub>, respectively. Temperature dependencies of selected bond distances and volumes of CsI<sub>9</sub>, RbI<sub>9</sub>, CsI<sub>12</sub>, PbI<sub>6</sub>-polyhedrons in CsPbI<sub>3</sub> and RbPbI<sub>3</sub> structures are presented in figures 5 and 6, respectively. No anomalous behaviour in those dependences can be observed. Pb-I, Pb-Pb, Cs/Rb-Cs/Rb, Cs/Rb-Pb and I-I distances are very close in both compounds and exhibit quite similar behaviour upon temperature increase. The main difference in 9-fold iodine environment of alkaline ion is that one of the Rb-I3 distances is 7.4% shorter than the longest one, whereas corresponding Cs-I3 distance in CsPbI<sub>3</sub> is only 2.8% shorter. A decrease in the volume of the PbI<sub>6</sub> polyhedron through the orthorhombic↔cubic phase transition is clearly visible in CsPbI<sub>3</sub> (figure 6).

## Discussion

A minor difference of 0.2% between our (854.23(12) Å<sup>3</sup>) and the literature (852.33 Å<sup>3</sup> [5]) value of the RbPbI<sub>3</sub> cell volume at room temperature can be due to the

different experimental setups and technique used, whereas the value of  $892.71 \text{ \AA}^3$  [4] for the  $\text{CsPbI}_3$  cell volume at room temperature agrees well with the  $892.66(4) \text{ \AA}^3$  value resulting from our studies.

Before melting,  $\text{CsPbI}_3$  undergoes a reversible orthorhombic-to-cubic phase transition *via* a two-phase region ( $Pnma \xrightarrow{563K} Pnma + Pm\bar{3}m \xrightarrow{602K} Pm\bar{3}m$ ) with a large discontinuous volume change of about 6.9%. This is a very strong indication for the first order phase transition in  $\text{CsPbI}_3$ . In contrast to  $\text{CsPbI}_3$ , no transition into the high-temperature modification was revealed for  $\text{RbPbI}_3$ . An attempt to detect the high-temperature polymorphic modification for rubidium triiodoplumbate has already been made [5] but it was not successful as well. An analysis of available literature data on high-temperature investigations of compounds which are isostructural to  $\text{CsPbI}_3$  ( $\text{TiMnI}_3$  and  $\text{TiFeI}_3$  [10],  $\text{InCdBr}_3$  [11],  $\text{InFeBr}_3$  and  $\text{InMnBr}_3$  [12],  $\text{KMnCl}_3$  and  $\text{TiMnCl}_3$  [13],  $\text{KMnBr}_3$  [14]) has shown the existence of phase transformations in  $\text{InFeBr}_3$ ,  $\text{KMnCl}_3$  and  $\text{TiMnCl}_3$  in addition to the melting. Crystals of  $\text{KMnCl}_3$  and  $\text{TiMnCl}_3$  transform immediately to the perovskite structures upon heating, whereas the reverse phase transitions need comparatively longer period of time [13]. Our experiment does not show any delay in the reverse phase transition for  $\text{CsPbI}_3$  (the furnace was cooled to room temperature after heating up to 687 K in about 10 minutes and the pattern from  $\text{CsPbI}_3$  after temperature treatment was collected in approximately 5 minutes).

The averaged Pb-I distance in  $\text{PbI}_6$ -octahedra increases from  $3.244 \text{ \AA}$  at 298 K up to  $3.266 \text{ \AA}$  at 593 K for orthorhombic  $\text{CsPbI}_3$ , from  $3.144 \text{ \AA}$  at 609 K up to  $3.150 \text{ \AA}$  at 687 K for cubic  $\text{CsPbI}_3$  and from  $3.231 \text{ \AA}$  at 298 K up to  $3.247 \text{ \AA}$  at 634 K for orthorhombic  $\text{RbPbI}_3$ . The values for the averaged Pb-I distance are almost the same in both orthorhombic phases and appear to be shorter than the Pb-I distance ( $3.39 \text{ \AA}$ ) calculated from the sum of the Shannon ionic radii. The last fact may be related to polarizing influence of smaller  $\text{Pb}^{2+}$  cations on the iodine anion surrounding.

Reference [12] reports the existence of an  $\text{In}^+-\text{Br}^-$  distance which is about 20% longer than all the other distances in the  $\text{InBr}_9$ -polyhedra of  $\text{InFeBr}_3$ . Similar experimental data are available for  $\text{InMnBr}_3$  (single elongation of about 20%),  $\text{InCdBr}_3$  (~16%) and  $\text{RbCdBr}_3$  (~10%) and they have been explained on the basis of crystal and electronic structure considerations [11]. However, such an elongation is not pronounced for the distances in the 9-fold iodine surroundings of alkaline ions in caesium and

rubidium triiodoplumbates. The averaged alkaline-iodine distances increase from 3.958 Å at 298 K up to 4.007 Å at 593 K in CsPbI<sub>3</sub> and from 3.872 Å at 298 K up to 3.940 Å at 634 K in RbPbI<sub>3</sub>. Cs-I distances of the cubic perovskite phase of CsPbI<sub>3</sub> vary from 4.446 Å at 609 K up to 4.455 Å at 687 K. Furthermore, the averaged Cs-I distance in CsPbI<sub>3</sub> at room temperature is about 0.025 Å shorter than the calculated sum of caesium and iodine Shannon ionic radii (3.98 Å), whereas this is not faithfully for RbPbI<sub>3</sub> (averaged Rb-I distance of 3.872 Å is 0.042 Å longer than 3.83 Å value calculated from Shannon ionic radii). Hence, the 9-fold iodine environment of Cs<sup>+</sup> ion should be more bulged out in comparison to those of Rb<sup>+</sup>; and these conditions may define the existence of a polymorphic phase transition in CsPbI<sub>3</sub> or its absence in RbPbI<sub>3</sub>. In order to check our assumption, the differences between the experimentally determined averaged cation-anion distance and the calculated one using the corresponding Shannon radii were estimated for other compounds of the NH<sub>4</sub>CdCl<sub>3</sub> structure type. Similar to caesium triiodoplumbate, the calculated K<sup>+</sup>-Br<sup>-</sup> distances in KMnBr<sub>3</sub>, and the Tl<sup>+</sup>-I<sup>-</sup> distances in TlMnI<sub>3</sub> and TlFeI<sub>3</sub> appear to be larger than those derived from diffraction studies. However, no high-temperature phase transitions (except the sample melting) were detected for these compounds [10, 14]. We could not find any evidence for relation between an existence/absence of polymorphic phase transitions in CsPbI<sub>3</sub>/RbPbI<sub>3</sub> and the difference in experimentally determined alkali-iodine distances and the ones calculated from the sum of ionic radii.

### Conclusions

The structural parameters of improved accuracy were derived for caesium triiodoplumbate by means of synchrotron powder diffraction experiments and the Rietveld refinement technique. CsPbI<sub>3</sub> crystallizes in the NH<sub>4</sub>CdCl<sub>3</sub>-structure, whereas references [15, 16] pointed out distorted perovskite structures for CsPbCl<sub>3</sub> and CsPbBr<sub>3</sub> (see also references therein [16]). We can therefore confirm the assumption of [17], where a different structure of CsPbI<sub>3</sub> was suggested to be responsible for considerable changes of optical properties in the CsPbX<sub>3</sub> (X=Cl, Br, I) series.

A pronounced difference in the high-temperature behaviour of the CsPbI<sub>3</sub> and RbPbI<sub>3</sub> structures was observed: CsPbI<sub>3</sub> undergoes a first order reversible phase transition whereas no polymorphic transformations were detected for RbPbI<sub>3</sub> before melting. To our knowledge, the conditions that define the presence or absence of a similar high temperature phase transitions in compounds of the NH<sub>4</sub>CdCl<sub>3</sub>-structure

type are not yet clear. However, further systematic high temperature investigations on  $\text{Cs}_x\text{Rb}_{1-x}\text{PbI}_3$ ,  $\text{InMn}_x\text{Fe}_{1-x}\text{Br}_3$  and  $\text{InCd}_x\text{Fe}_{1-x}\text{Br}_3$  solid solutions, which are envisaged in the near future, could probably contribute to a better understanding of the relationships between structure parameters and the occurrence/absence of phase transitions in this structure type.

### Acknowledgments

The authors are indebted to Dr. G. Stryganyuk (HASYLAB/DESY) and Dr. A. Senyshyn (TU Darmstadt/TU Munich, FRM-II) for the critical manuscript reading as well as to Prof. L. Vasylechko (Lviv Polytechnic National University, Ukraine). We are also grateful to Dr. Th. Vad (TU Dresden) for assisting in the preparation of the manuscript. The HASYLAB/DESY support of Powder Diffractometer at beamline B2 and financial support from the Helmholtz Association of National Research Centres (grant number VH-VI 102) are gratefully acknowledged.

### References

- [1] A. S. Voloshinovskiy, S. V. Myagkota, N. S. Pidzyrailo, Z. A. Khapko, *Ukr. Fiz. Zh.* 32 (1987) 685–687 (in Russian).
- [2] S. V. Myagkota, *Opt. Spectrosc.* 87 (1999) 290–294.
- [3] S. Zazubovich, *Radiat. Meas.* 33 (2001) 699–704.
- [4] C. K. Møller, *Mat. Fys. Medd. Dan. Vid.* 32 (1959) 1–18.
- [5] H. J. Haupt, F. Huber and H. Preut, *Z. anorg. allg. Chem.* 408 (1974) 209–213.
- [6] M. Knapp, C. Baetz, H. Ehrenberg, H. Fuess, *J. Synchrotron Radiat.* 11 (2004) 328–334.
- [7] M. Knapp, V. Joco, C. Baetz, H. Brecht, A. Berghaeuser, H. Ehrenberg, H. von Seggern and H. Fuess, *Nucl. Instrum. Meth. A* 521 (2004) 565–570.
- [8] T. Roisnel, J. Rodriguez-Carvajal, *Mater. Sci. Forum* 378–381 (2001) 118–123.
- [9] J. Hutton, R. J. Nelmes, G. M. Meyer, V. R. Eiriksson, *J. Phys. C Solid State* 12 (1979) 5393–5410; M. Sakata, T. Nishiwaki, J. Harada, *J. Phys. Soc. Jpn.* 47 (1979) 232–233.
- [10] H.W. Zandbergen, *J. Solid State Chem.* 37 (1981) 189–203.
- [11] R. Dronskowski, *J. Solid State Chem.* 116 (1995) 45–52.



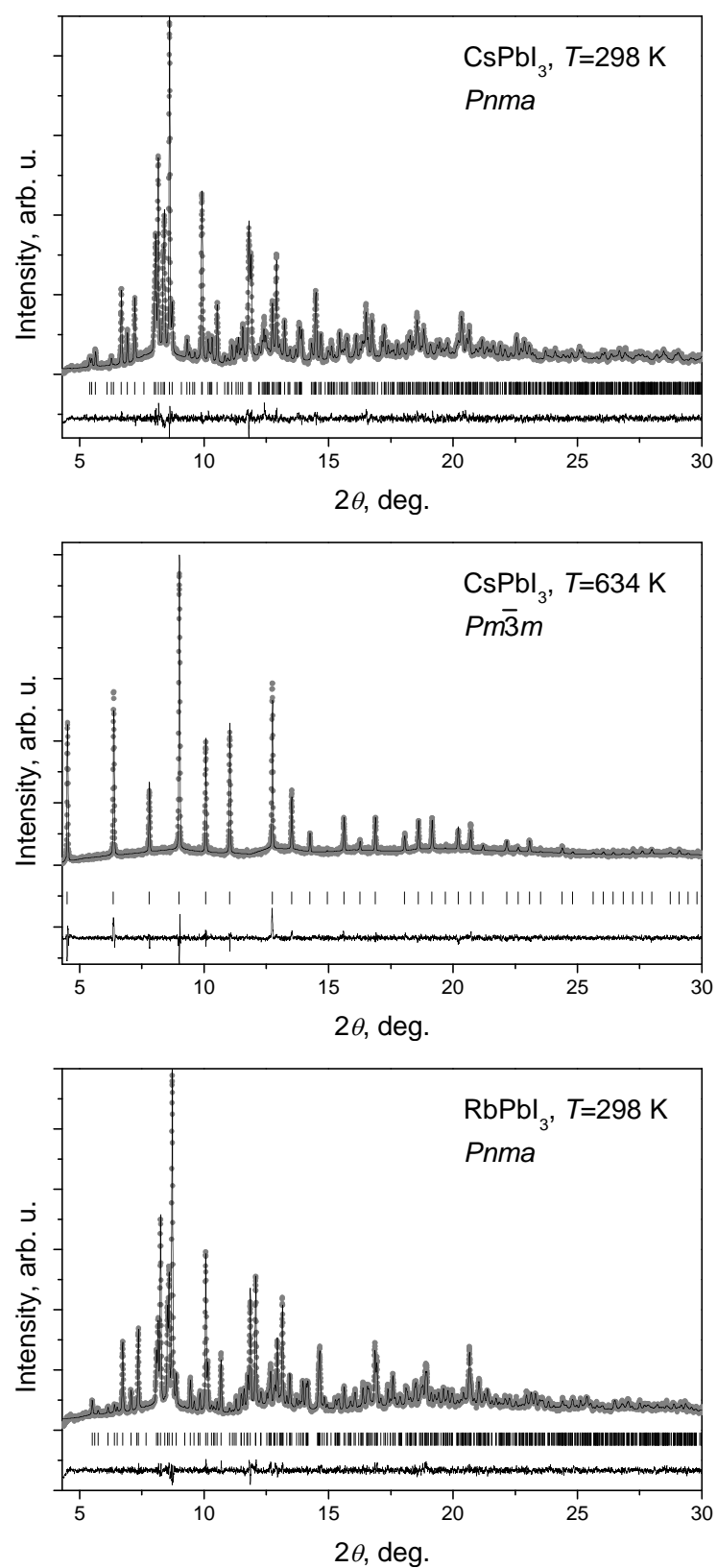
- [12] R. Dronskowski, *Inorg. Chem.* 33 (1994) 5927–5933.
- [13] A. Horowitz, M. Amit, J. Makovsky, L. Ben Dor, Z. H. Kalman, *J. Solid State Chem.* 43 (1982) 107–125.
- [14] H.-J. Seifert, E. Dau, *Z. anorg. allg. Chem.* 391 (1972) 302–312.
- [15] Y. Fujii, S. Hoshino, Y. Yamada, G. Shirane, *Phys. Rev. B* 9 (1974) 4549-4559.
- [16] K. Nitsch, V. Hamplova, M. Nikl, K. Polak, M. Rodova, *Chem. Phys. Lett.* 258 (1996) 518-522.
- [17] F. Somma, M. Nikl, K. Nitsch, P. Fabeni, G.P. Pazzi, *J. Lumin.* 94-95 (2001) 169-172.

Table 1: Refined structural parameters and R-factors of CsPbI<sub>3</sub> and RbPbI<sub>3</sub>

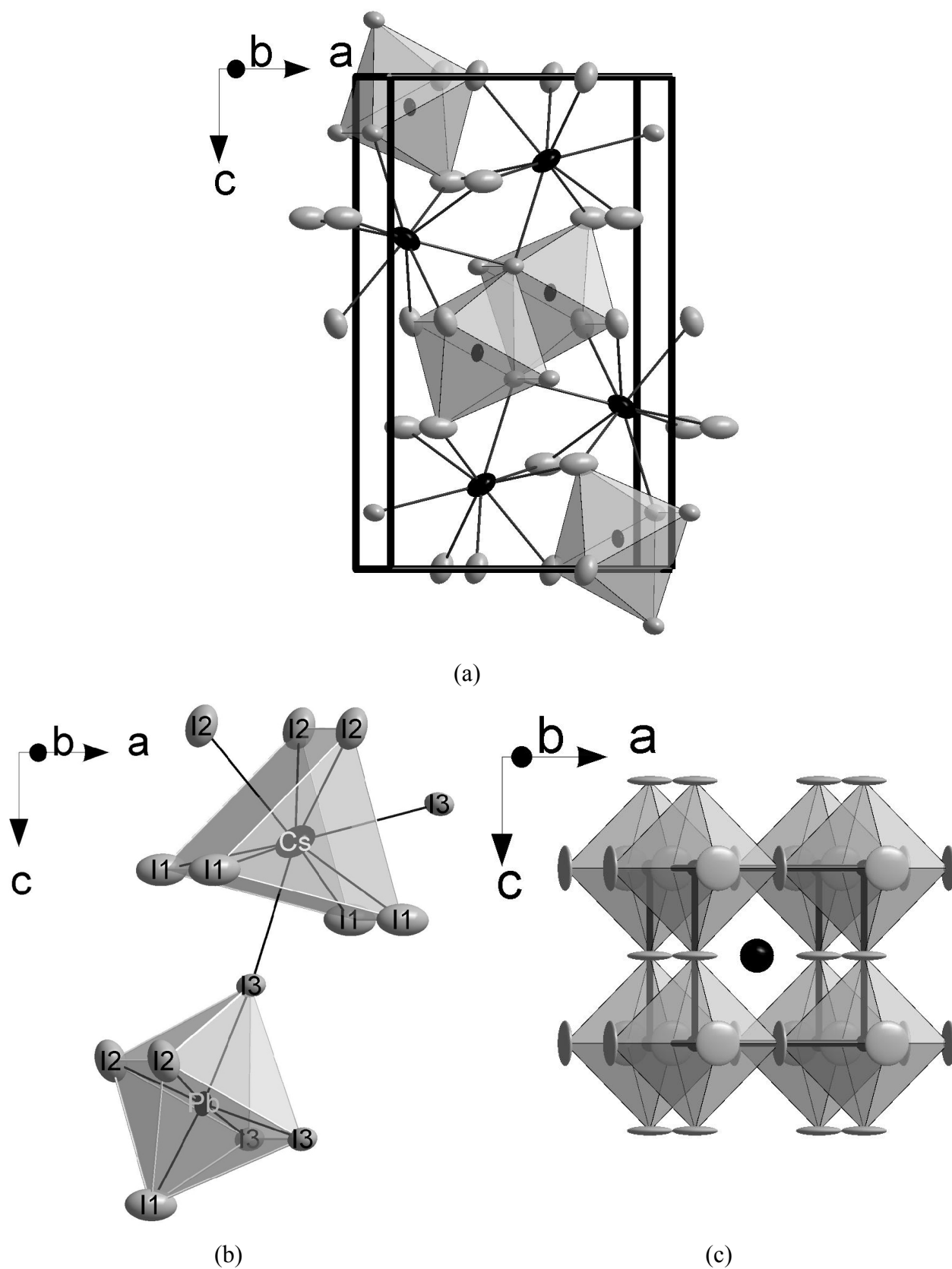
		CsPbI <sub>3</sub>		RbPbI <sub>3</sub>	
Temperature (K)		298	634	298	634
Space group		<i>Pnma</i>	<i>Pm</i> $\bar{3}$ <i>m</i>	<i>Pnma</i>	<i>Pnma</i>
	<i>a</i> (Å)	10.4581(3)	6.2894(19)	10.2761(9)	10.4200(4)
	<i>b</i> (Å)	4.80171(13)	—	4.7793(4)	4.84098(16)
	<i>c</i> (Å)	17.7761(5)	—	17.3933(12)	17.6145(5)
	<i>V</i> (Å <sup>3</sup> ) / <i>Z</i>	892.66(4) / 4	248.784(13) / 1	854.23(12) / 4	888.53(5) / 4
Cs/Rb	<i>site</i>	4( <i>c</i> )	1( <i>b</i> )	4( <i>c</i> )	4( <i>c</i> )
	<i>x/a</i>	0.4156(3)	½	0.4166(5)	0.4159(6)
	<i>y/b</i>	¼	½	¼	¼
	<i>z/c</i>	0.82924(19)	½	0.8263(3)	0.8264(4)
	<i>U</i> <sub>iso</sub> (Å <sup>2</sup> )	0.025(3)	0.159(2)	0.033(5)	0.092(9)
	<i>U</i> <sub>11</sub>	0.024(3)	—	0.044(5)	0.104(9)
	<i>U</i> <sub>22</sub>	0.032(3)	—	0.034(5)	0.107(10)
	<i>U</i> <sub>33</sub>	0.017(3)	—	0.020(4)	0.064(8)
	<i>U</i> <sub>13</sub>	-0.008(2)	—	0.003(3)	0.000(5)
Pb	<i>site</i>	4( <i>c</i> )	1( <i>a</i> )	4( <i>c</i> )	4( <i>c</i> )
	<i>x/a</i>	0.16049(18)	0	0.1662(2)	0.1662(3)
	<i>y/b</i>	¼	0	¼	¼
	<i>z/c</i>	0.06185(11)	0	0.06001(11)	0.06080(17)
	<i>U</i> <sub>iso</sub> (Å <sup>2</sup> )	0.0111(10)	0.0392(9)	0.0172(16)	0.051(3)
	<i>U</i> <sub>11</sub>	0.0034(4)	—	0.0237(17)	0.061(3)
	<i>U</i> <sub>22</sub>	0.0201(15)	—	0.0215(16)	0.046(3)
	<i>U</i> <sub>33</sub>	0.0097(10)	—	0.0065(14)	0.047(3)
	<i>U</i> <sub>13</sub>	0.0008(14)	—	-0.0024(15)	-0.009(3)
I1	<i>site</i>	4( <i>c</i> )	3( <i>d</i> )	4( <i>c</i> )	4( <i>c</i> )
	<i>x/a</i>	0.2997(3)	½	0.3068(3)	0.3048(4)
	<i>y/b</i>	¼	0	¼	¼
	<i>z/c</i>	0.2127(2)	0	0.2149(2)	0.2126(3)
	<i>U</i> <sub>iso</sub> (Å <sup>2</sup> )	0.025(3)	0.194(3)	0.027(3)	0.071(5)
	<i>U</i> <sub>11</sub>	0.045(3)	0.015(2)	0.039(3)	0.092(5)
	<i>U</i> <sub>22</sub>	0.015(3)	0.283(3)	0.022(3)	0.069(5)
	<i>U</i> <sub>33</sub>	0.016(3)	0.283(3)	0.018(3)	0.052(5)
	<i>U</i> <sub>13</sub>	-0.001(2)	0	-0.011(3)	-0.023(5)
I2 in 4 <i>c</i>	<i>site</i>	4( <i>c</i> )	—	4( <i>c</i> )	4( <i>c</i> )
	<i>x/a</i>	0.3355(3)	—	0.3396(4)	0.3363(5)
	<i>y/b</i>	¾	—	¾	¾
	<i>z/c</i>	0.99790(19)	—	0.99020(18)	0.9910(2)
	<i>U</i> <sub>iso</sub> (Å <sup>2</sup> )	0.021(3)	—	0.025(3)	0.075(6)
	<i>U</i> <sub>11</sub>	0.016(2)	—	0.020(3)	0.100(6)
	<i>U</i> <sub>22</sub>	0.019(3)	—	0.029(3)	0.068(5)
	<i>U</i> <sub>33</sub>	0.028(3)	—	0.026(3)	0.056(6)
	<i>U</i> <sub>13</sub>	-0.005(2)	—	0.007(3)	0.002(4)
I3	<i>site</i>	4( <i>c</i> )	—	4( <i>c</i> )	4( <i>c</i> )
	<i>x/a</i>	0.0331(3)	—	0.0272(3)	0.0252(4)
	<i>y/b</i>	¼	—	¼	¼
	<i>z/c</i>	0.88541(19)	—	0.8837(2)	0.8860(3)
	<i>U</i> <sub>iso</sub> (Å <sup>2</sup> )	0.015(3)	—	0.018(3)	0.051(5)
	<i>U</i> <sub>11</sub>	0.013(2)	—	0.015(3)	0.039(5)
	<i>U</i> <sub>22</sub>	0.022(3)	—	0.035(3)	0.065(5)
	<i>U</i> <sub>33</sub>	0.009(3)	—	0.003(2)	0.050(5)
	<i>U</i> <sub>13</sub>	0.001(2)	—	-0.005(2)	-0.006(3)
R <sub>Bragg</sub> (%) / R <sub>F</sub> (%) / χ <sup>2</sup>		5.6/6.1/10.1	6.4/6.3/11.5	4.9/5.4/9.3	6.0/9.6/8.2

Table 2: Comparison of bound distances and angles of CsPbI<sub>3</sub> and RbPbI<sub>3</sub>

	RbPbI <sub>3</sub> at 298 K	RbPbI <sub>3</sub> at 634 K	CsPbI <sub>3</sub> at 298 K	CsPbI <sub>3</sub> at 634 K
Cs/Rb - I1 × 2	3.7747(47)	3.8476(59)	3.8892(37)	Cs - I × 12 4.4473
Cs/Rb - I1 × 2	3.8430(48)	3.8928(63)	3.8968(35)	Cs - Pb × 8 5.4468
Cs/Rb - I2 × 2	3.8068(48)	3.8684(62)	3.9312(38)	Cs - Cs × 6 6.2894
Cs/Rb - I3 × 1	3.8164(62)	3.9072(87)	4.0086(47)	Pb - I × 6 3.1447
Cs/Rb - I2 × 1	4.0530(63)	4.1266(80)	4.0271(46)	Pb - Pb × 6 6.2894
Cs/Rb - I3 × 1	4.1327(60)	4.2053(76)	4.1230(45)	I - I × 8 4.4473
⟨Cs/Rb - I <sub>9</sub> ⟩	3.872	3.940	3.958	I - I × 6 6.2894
Cs/Rb - Pb × 1	4.8138(56)	4.8815(75)	4.9209(38)	
Cs/Rb - Pb × 2	5.2822(50)	5.3353(68)	5.3842(35)	
Cs/Rb - Pb × 2	5.2873(49)	5.3644(63)	5.4006(33)	
Pb - I1 × 1	3.0568(39)	3.0388(59)	3.0513(40)	
Pb - I2 × 2	3.2162(29)	3.2415(38)	3.2259(25)	
Pb - I3 × 2	3.2576(26)	3.2733(36)	3.2775(25)	
Pb - I3 × 1	3.3822(39)	3.4133(59)	3.4076(39)	
⟨Pb - I <sub>6</sub> ⟩	3.231	3.247	3.244	
Pb - Pb × 2	4.6550(24)	4.7371(38)	4.6763(23)	
I1 - I3 × 2	4.1525(39)	4.2805(59)	4.2717(40)	
I1 - I2 × 2	4.5881(40)	4.6047(54)	4.5259(42)	
I1 - I3 × 2	4.5142(38)	4.5474(53)	4.5738(39)	
I1 - I2 × 1	5.0217(47)	5.1189(64)	5.2632(49)	
I2 - I2 × 2	4.0880(47)	4.1967(60)	4.1962(36)	
I2 - I3 × 1	4.3574(50)	4.3445(66)	4.3775(45)	
I2 - I3 × 2	4.4110(42)	4.4491(55)	4.4457(38)	
I3 - I3 × 2	4.7363(42)	4.7212(64)	4.7792(41)	
I1 - Cs/Rb - I1 × 1	78.538	77.966	76.065	
I1 - Cs/Rb - I1 × 1	76.884	76.894	76.241	
I1 - Cs/Rb - I1 × 2	87.78(10)	87.938(126)	87.714(64)	
I1 - Cs/Rb - I1 × 2	138.445	138.274	136.119	
I1 - Cs/Rb - I2 × 2	71.667(1)	70.442	69.641(1)	
I1 - Cs/Rb - I2 × 2	140.047(1)	140.430	141.320(1)	
I1 - Cs/Rb - I2 × 2	84.337(93)	84.397(125)	86.127(64)	
I1 - Cs/Rb - I2 × 2	134.151	133.599	133.235	
I1 - Cs/Rb - I2 × 2	82.058(77)	82.531(118)	84.598(62)	
I1 - Cs/Rb - I2 × 2	129.96	130.400	131.29	
I1 - Pb - I2 × 2	93.975(3)	92.253	92.234(6)	
I1 - Pb - I3 × 2	91.214(10)	92.103(7)	92.485(5)	
I1 - Pb - I3 × 1	176.754(110)	177.161(166)	174.516(110)	
I2 - Pb - I2 × 1	95.956	96.613	96.189	
I2 - Pb - I3 × 2	84.608(46)	83.651(68)	84.612(42)	
I2 - Pb - I3 × 2	174.727(1)	173.598	175.179(1)	
I2 - Pb - I3 × 2	83.862(2)	83.868(3)	84.115(2)	
I3 - Pb - I3 × 2	90.993(12)	89.807(57)	91.247(10)	



**Figure 1.** The results of Rietveld refinements: points are experimental data, the lines are calculated profiles and the lower curves their differences. Tick marks show the calculated positions of  $\text{CsPbI}_3$  and  $\text{RbPbI}_3$  reflections.



**Figure 2.** The structures of  $\text{CsPbI}_3$  at room temperature (a) and at  $T=634$  K (c). (b) – iodine surroundings of alkaline and  $\text{Pb}^{2+}$  cations. Plots (a), (b) and (c) show the thermal ellipsoids at the 100%, 100% and 50% probability level, respectively.

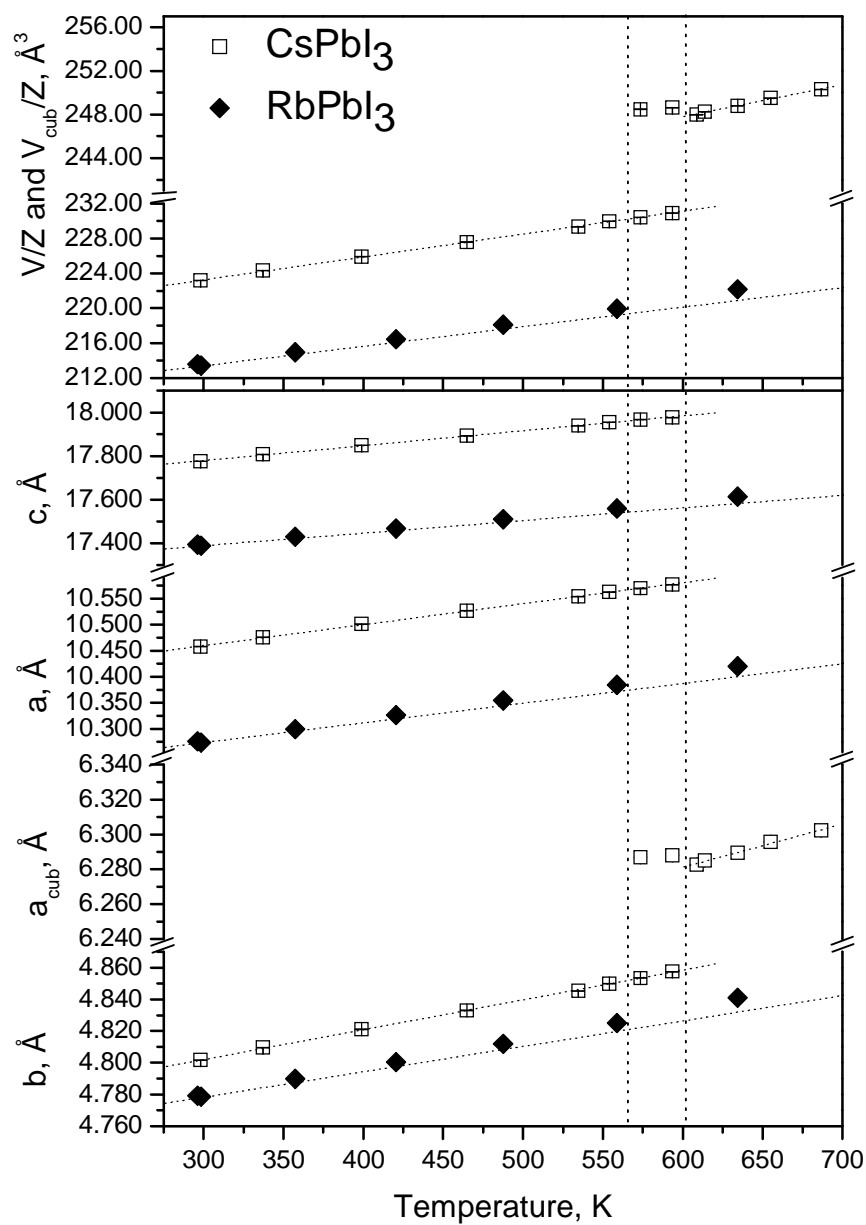


**Figure 3.** Temperature evolution of cell dimensions of CsPbI<sub>3</sub> and RbPbI<sub>3</sub>. Two dotted vertical lines represent the boundaries of mixed  $Pnma + Pm\bar{3}m$  region in CsPbI<sub>3</sub>.

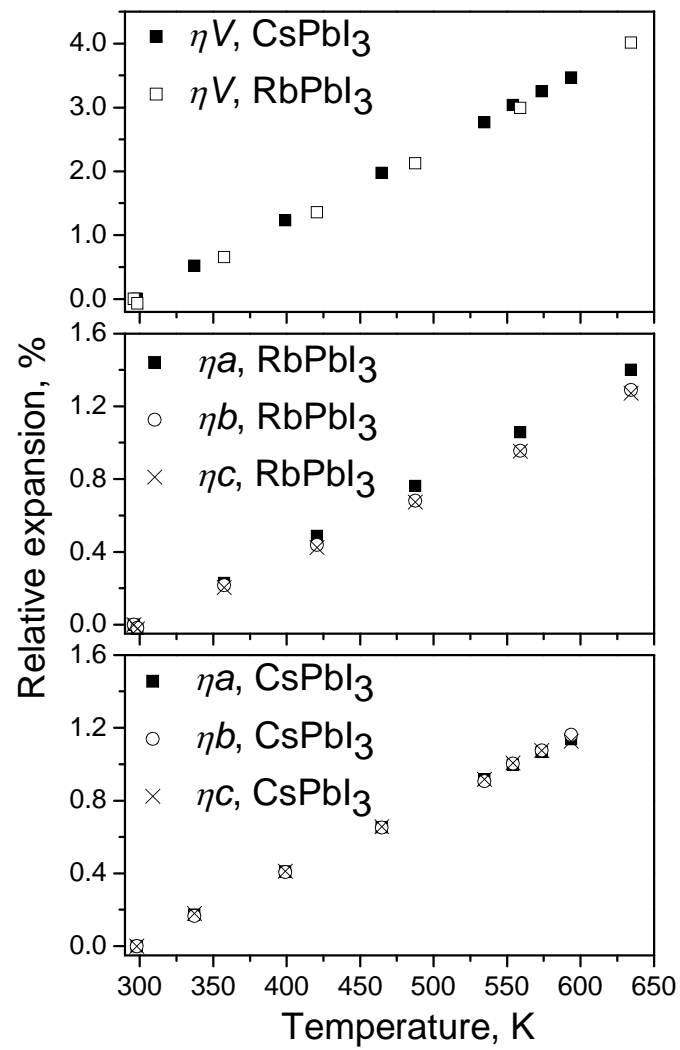


**Figure 4.** Relative expansions in CsPbI<sub>3</sub> and RbPbI<sub>3</sub> structures.

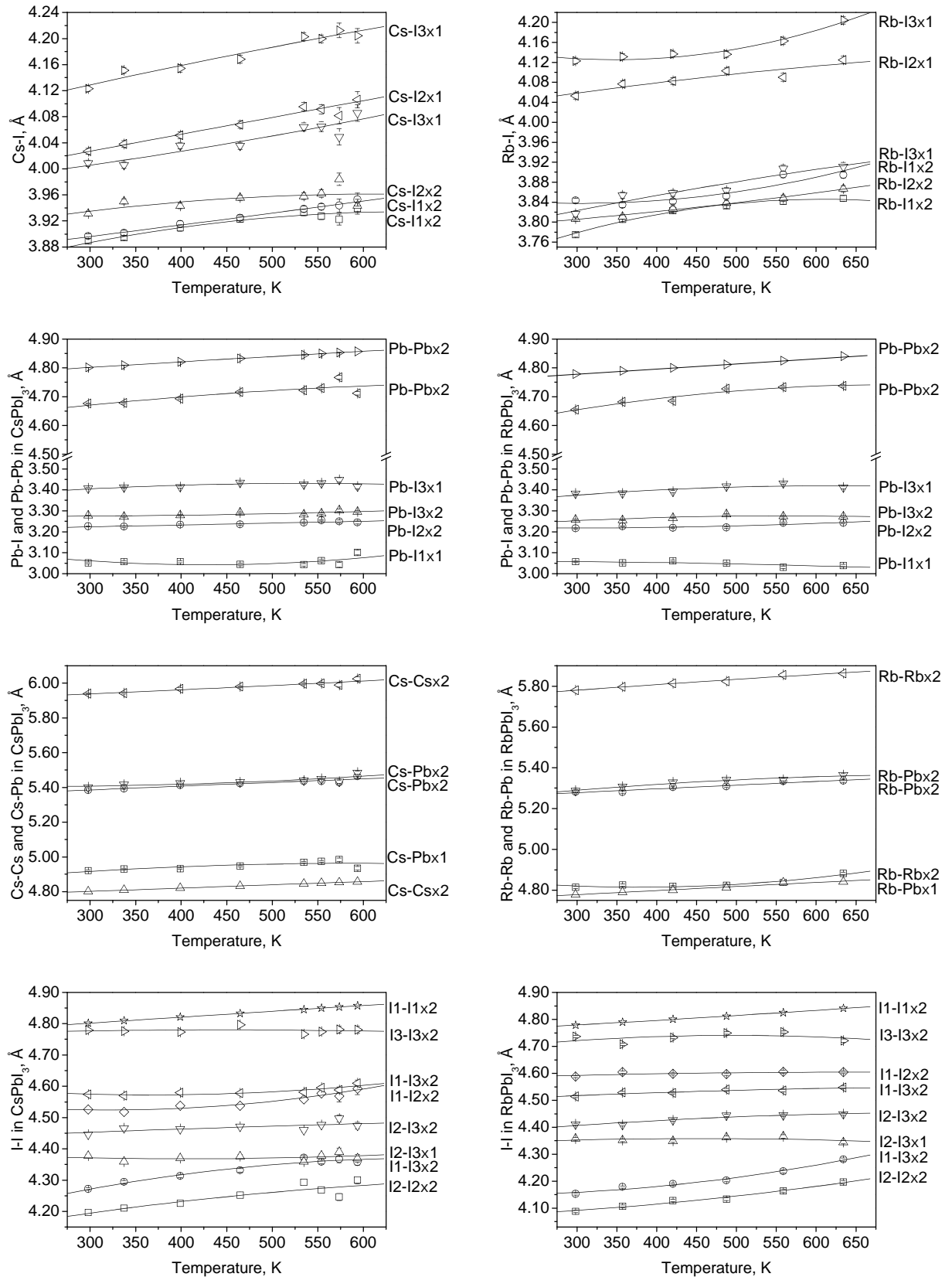


**Figure 5.** Temperature dependencies of selected bond distances in  $\text{CsPbI}_3$  and  $\text{RbPbI}_3$  structures. Experimental data points were fitted by second-order polynomials.



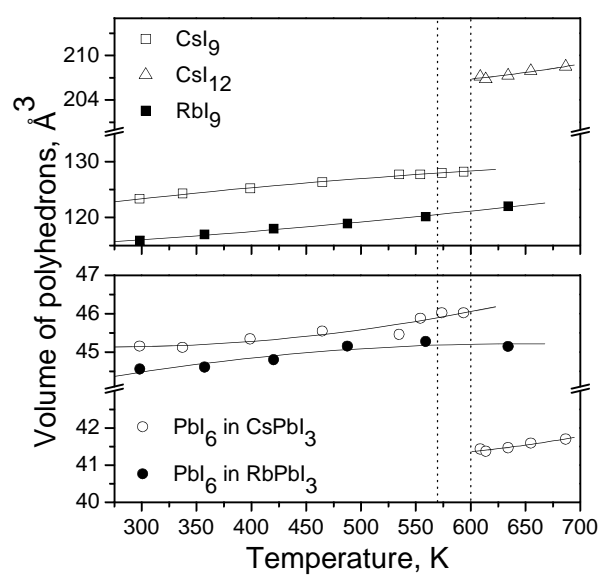


**Figure 6.** Temperature dependencies of volumes of CsI<sub>12</sub>, CsI<sub>9</sub>, PbI<sub>6</sub> and RbI<sub>9</sub> polyhedrons. Data points were fitted by second-order polynomials.